Electronic Supplementary Material (ESI) for New Journal of Chemistry.

Platinum(II) N-heterocyclic carbene *cis* and *trans* isomers: synthesis, characterization and biological activity

Carolina Rivera,[a] Héctor A. Bacilio-Beltrán,[a] Ana M. Puebla-Pérez,[b] Irma I. Rangel-Salas,[a] José G. Alvarado-Rodríguez,[c] Roberto Flores-Moreno,[a] Gilberto Velázquez-Juárez,[a] A. Aarón Peregrina-Lucano,[b] Elvia Becerra-Martínez,[d] Jaime Valdez-Ruvalcaba, José E. Rubio,[e] Sara A. Cortés-Llamas[a]*

[a] Departamento de Química, [b] Departamento de Farmacobiología; Centro Universitario de Ciencias Exactas e Ingenierías, Universidad de Guadalajara, Blvd. Marcelino García Barragán #1421, esq. Olímpica, C.P. 44430 Guadalajara, Jalisco, México.

[c] Universidad Autónoma del Estado de Hidalgo. Unidad Universitaria, km 4.5 Carretera Pachuca-Tulancingo, C.P. 42184, Mineral de la Reforma, Hidalgo, México.

[d] Centro de Nanociencias y Micro y Nanotecnologías, Instituto Politécnico Nacional. Unidad Profesional "Adolfo López Mateos", Luis Enrique Erro S/N, Zacatenco C. P. 07738, México, D. F.

[e] Department of Electronics, ETSIT, University of Valladolid, Paseo Belen 15, Valladolid 47011, Spain.

Contents

Experimental section

Experimental Section

General Information

All chemicals were obtained from Sigma–Aldrich. [Pt(*S*-dmso)$_2$Cl$_2$] and the masked carbene 1,3-dimethylimidazolium-2-carboxylate were synthesized according to the literature.[1,2] 1,3-Dimethylimidazolium-2-carboxylate was stored under a N_2 atmosphere to prevent hydration. ^{1}H and ^{13}C NMR spectra were obtained using a Bruker Ascend 750 MHz spectrometer. Single crystal X-ray diffraction data of Compounds **1a** and **1b** were collected at room temperature on an Oxford Diffraction Gemini CCD diffractometer with graphite-monochromated Mo-Kα radiation (λ = 0.71073). Data were integrated, scaled, sorted, and averaged using the CrysAlis software package. Using Olex2,[3] the structures were solved with the ShelXT structure solution program using Direct Methods and refined with the ShelXL[4] refinement package through least squares minimization. All nonhydrogen atoms were refined anisotropically. The positions of the hydrogen atoms were fixed with a common isotropic displacement parameter. UV–vis absorption spectra were recorded at room temperature using a Thermo Scientific Genesys10S spectrometer. Mass spectra were obtained by LC/MSD TOF with APCI as ionization source in an Agilent G1969A. XPS spectra was obtained using an 1486.7 eV Al K-α monochromatic source of 250W and 12.5 kV. The detector is 1D DLD with Phoibos 150 analyzer. Operation pressure was 4.79×10−9 milibar. Charge compensator is a Flood gun operated at 20 microamperes and 3 eV.

Synthesis of cis-[Pt(^{Me}NHC)$_2$Cl$_2$] (**1a**)

100 mg (0.23 mmol) of [Pt(*S*-dmso)$_2$Cl$_2$] and 66 mg (0.47 mmol) of 1,3 dimethylimidazolium-2-carboxylate were dissolved in a vial containing 10 mL of acetonitrile. The reaction was stirred overnight at 60 °C and then filtered through a 0.2-µm-pore-size filter, and the solvent was removed. The white solid was washed with diethyl ether and dried. Crystals were obtained from a concentrated solution in acetonitrile at 80 °C, and 15 mL of hexanes were dropwise added. Yield: 88%; decomposition temperature: 280 °C, white solid; ^{1}H NMR ($CDCl_3$, 750 MHz, δ ppm): 6.83 (s, 4H, C*H*=C*H*), 3.95 (s, 12H, CH_3); ^{13}C NMR ($CDCl_3$, 188 MHz, δ ppm): 165.27 (N-*C*-N), 121.63 (*C*H=*C*H), 37.46 (*C*H_3); ESI-MS (m/z): 423.0 [Pt(^{Me}NHC)$_2$Cl]$^+$.

Synthesis of trans-[Pt(^{Me}NHC)$_2$Cl$_2$] (**1b**)

100 mg (0.24 mmol) of $K_2[PtCl_4]$ and 130 mg (0.92 mmol) of 1,3-dimethylimidazolium-2-carboxylate were added to a flask containing 15 mL of acetonitrile.[1] The reaction was stirred overnight at 60 °C and then filtered through a 0.2-µm-pore-size filter, and the solvent was removed. The yellow solid was washed with methanol and dried. Crystals were obtained by slow evaporation at 45 °C from a concentrated solution in acetonitrile. Yield: 85%; decomposition temperature: 300 °C, yellow solid; ^{1}H NMR ($CDCl_3$, 750 MHz MHz, δ ppm): 6.81 (s, 4H, C*H*=C*H*), 4.13 (s, 12H, CH_3); ^{13}C NMR ($CDCl_3$, 188 MHz, δ ppm): 167.27 (N-*C*-N), 121.39 (*C*H=*C*H), 36.94 (*C*H_3); ESI-MS (m/z): 423.0 [Pt(^{Me}NHC)$_2$Cl]$^+$, 501.0 [Pt (^{Me}NHC)$_2$Cl(H_2O)$_2$(ACN)]$^+$.

[1] For the synthesis of **1b** four equivalents of the ^{Me}NHC ligand favor the precipitation of the pale yellow solid. If two equivalents are used, a darker dense fluid is commonly obtained.

Computational details

Density functional theory (DFT) calculations were performed using a modified version of the deMon2k software package.[5,6] Theory level corresponds to auxiliary density functional theory (ADFT) with the PBE exchange-correlation functional[7,8] but using auxiliary densities for the computation of the exchange correlation energy functional.[9] TZVP[10] basis set was employed for the small atoms while LANL2DZ[11] basis and effective core potential (ECP) were used for platinum. Handling of ECP integrals was made with the half-numerical integration of pseudopotential integrator.[12] Auxiliary basis sets GEN-A2* were generated automatically as previously described.[12–15] Adaptive numerical integration grid of quality MEDIUM was employed.[16]

Cell cultures and cytotoxic studies

Prior to subjecting complexes **1a** and **1b** to biological tests, we confirmed their relative stability under physiological conditions. Since both complexes were obtained from nonaqueous solutions (MeCN), it was relevant to test their stability in aqueous media. Thus, their stability in the culture medium (RPMI 1640 and MEM) was studied by UV−vis spectroscopy. The time-dependent absorption spectra in the characteristic region displayed a minimum change (<8%) over the course of 30 h. Analogously, both compounds were also tested in PBS adjusted to a pH of 7.1±0.2 to confirm their stability in phosphates. Both tests resulted in clear solutions, and no particles or suspensions were formed.

Cell culture was performed using RPMI-1640 (Sigma–Aldrich) for HeLa (ATCC CCL-2) and L-5178Y cell lines and MEM (Sigma–Aldrich) for Caco-2 (ATCC HTB-37) cells in media containing 10% and 20% fetal bovine serum (Gibco), respectively, and 50 µg/mL gentamicin (Sigma Aldrich). Incubations were carried out at 37 °C, 5% CO_2 and relative humidity at the saturation point. Cells were seeded in flat-bottomed 96-well plates. A total of 20,000 cells/well were considered HeLa and L-5178Y cells, and 50,000 cells/well were considered Caco-2 cells. Plates were incubated for 24 h. Cytotoxicity was determined by MTT (3-(4,5-dimethyl 2-thiazolyl)-2,5-diphenyl-2H tetrazolium bromide) assay.[17,18] Stock solutions of the compounds were prepared in 0.5% DMSO aqueous solution and diluted in appropriate culture media at different concentrations: 0.01-100 µM; each well was filled to a final volume of 200 µL. *Cis*-platin (Sigma–Aldrich) and the precursor 1,3-dimethylimidazolium-2-carboxylate were used as positive and negative controls, respectively. DMSO at 0.5% v/v concentration was also added as control to discard solvent interferences. Undoped media culture was kept as a 100% viability control. Treated cells were incubated for 24 h.

MTT (Sigma–Aldrich) was prepared *in situ* at a 2 mg/mL concentration in PBS 7.2 (Sigma–Aldrich). Fifty microliters of this solution were added to the well plates, followed by 4 h of incubation. Subsequently, the culture media and MTT were discarded, and 100 µL of DMSO was poured to dissolve formazan. The optical density was measured at 540 nm. The reported IC_{50} values were determined by plotting the pM (-log µM) of compound concentration vs. cell viability from three independent experiments.

ROS Assay

ROS are generated due to the reduction of oxygen during aerobic respiration and by various enzymatic systems within the cell. In a 96-well flat clear bottom black culture plate, 20,000 HeLa cells (ATCC CCL-2) were placed with 90 µL of complete RPMI-1640 medium (10% fetal bovine serum and gentamicin to a final concentration of 50 µg/mL) for each well, cells were incubated for 24 hours at 37 °C and relative humidity at saturation.
After the incubation period, the following groups were tested; positive control H_2O_2, negative control RPMI-1640, *cis*-**1a**, *trans*-**1b**, *cis*-**1a** group/H_2O_2, and *trans*-**1b** group/H_2O_2. In all cases, RPMI-1640 medium was added in 10 µL doses to obtain a final concentration of 10 µM. It was incubated for 4 hours at 37 °C and relative humidity at saturation. After incubation, 100 µL of Master Reaction Mix prepared according to the Technical Bulletin of the Fluorometric Intracellular ROS Kit MAK144 (Sigma-Aldrich) were added to each well, prior to incubation for 1 hour at 37 °C and relative humidity at saturation. After the incubation period, each group was observed under a microscope using phase-contrast and the TRITC filter.

Antimicrobial activity study

The bacterial strains *B. subtilis, S. aureus* (Gram positive), *P. aeruginosa,* and *E. coli* (Gram negative) were obtained from the Molecular Biology Laboratory at the University of Guadalajara. The pure strains were cultured in Mueller-Hinton agar at 37 °C for 24 h. They were subcultured occasionally to maintain viability during the study period.

Preparation of Inoculum: Mueller-Hinton broth was prepared in a Schott bottle and sterilized. Aliquots of the Mueller-Hinton Cation Adjusted broth at 0.5 McFarland were placed into vials and inoculated with the strains. The inoculated bacterial cultures were kept overnight at 37 °C.

Disk Diffusion Method: The *in vitro* antibacterial activity of the samples was evaluated using the Mueller-Hinton agar disk diffusion method with determination of the diameter of inhibition zones in mm. *Escherichia coli* (ATCC 25922), *Staphylococcus aureus* (ATCC 25923), *Bacillus subtilis* (ATCC 633) and *Pseudomonas aeruginosa* (ATCC 27853) were used for the antibacterial effect assay. The bacterial suspension was prepared by making a saline suspension of isolated colonies selected from 18 to 24 h of tryptic soy agar plating. The suspension was adjusted to match the tube of 0.5-McFarland turbidity standard using spectrophotometry at 600 nm, which equals 1.5×10^8 colony-forming units/mL. The surface of the Mueller-Hinton agar was completely inoculated using a sterile swab, which was steeped in the prepared suspension of bacteria. Finally, the impregnated discs containing 50 µL of platinum complexes **1a** and **1b** were placed on inoculated agar and incubated at 37 °C for 24 h. After incubation, the diameters of the growth inhibition zones were measured. We considered inhibition zones larger than 10 mm to be positive.[19] It must be noted, however, that large inhibition zones do not necessarily reveal that a particular compound is the best antibacterial agent since this outcome may be attributed to the diffusion rate of the antibacterial agents and the number of bacterial isolates present in a certain amount of agar solution.[20] Amoxicillin, doxycycline, sulfamethoxazole, and gentamicin were used as the positive standards to control the sensitivity of the bacteria. All tests were performed in duplicate.

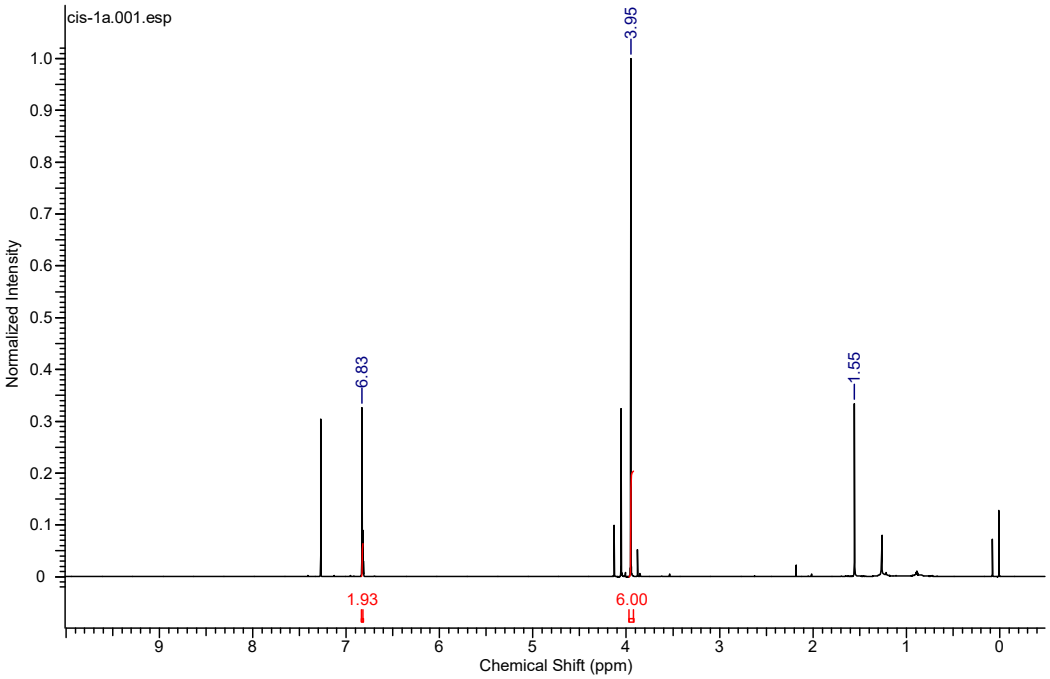
cis-1a.001.esp
3.95
6.83
1.55
1.93
6.00
Normalized Intensity
Chemical Shift (ppm)

1a

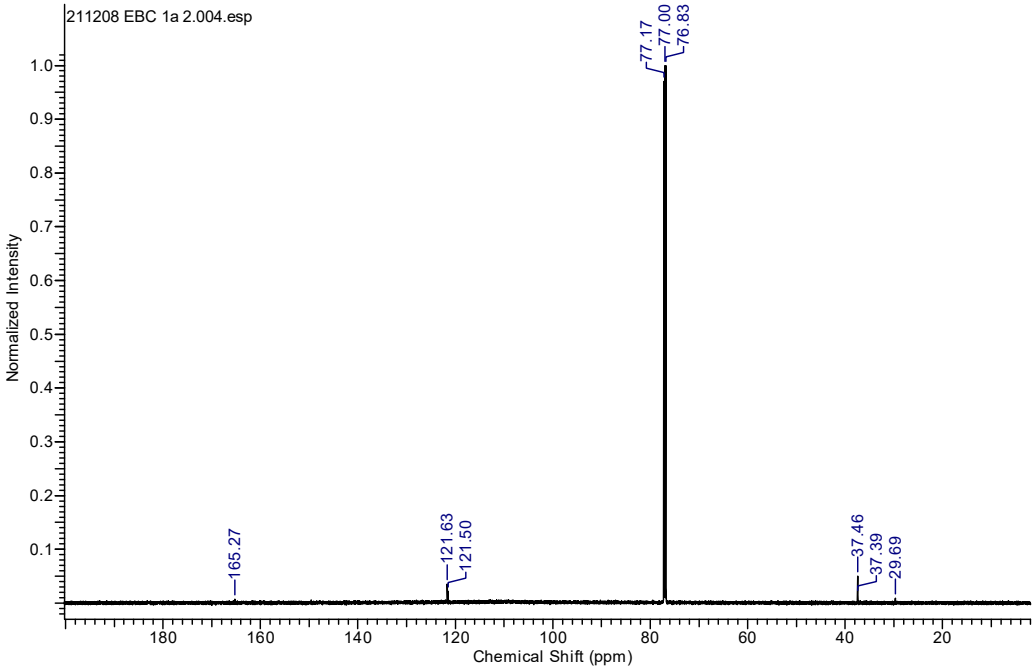
211208 EBC 1a 2.004.esp
77.17
77.00
76.83
165.27
121.63
121.50
37.46
37.39
29.69
Normalized Intensity
Chemical Shift (ppm)

1a

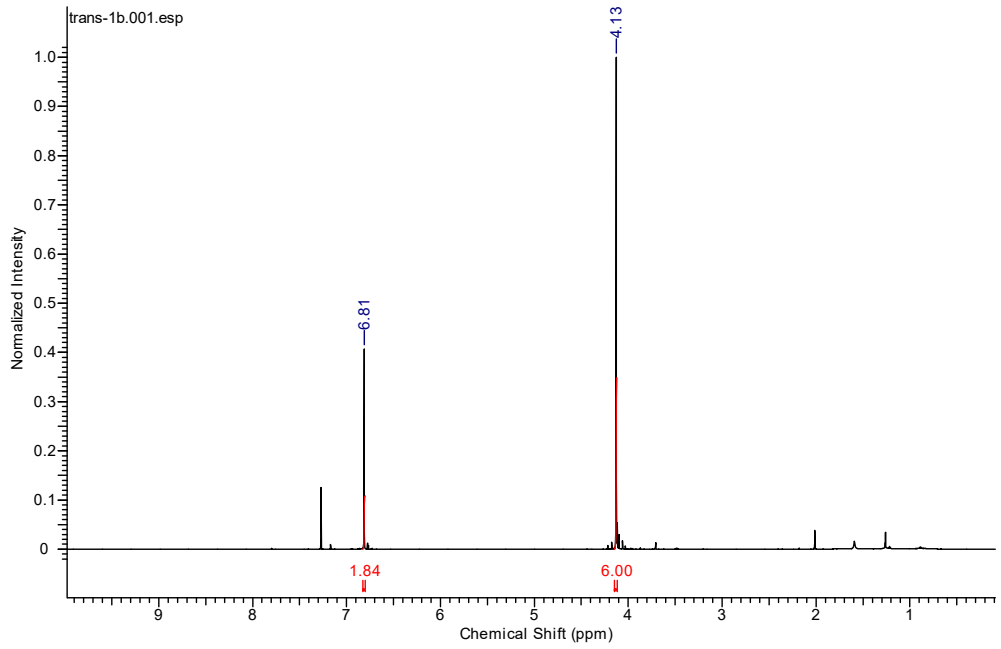

1b

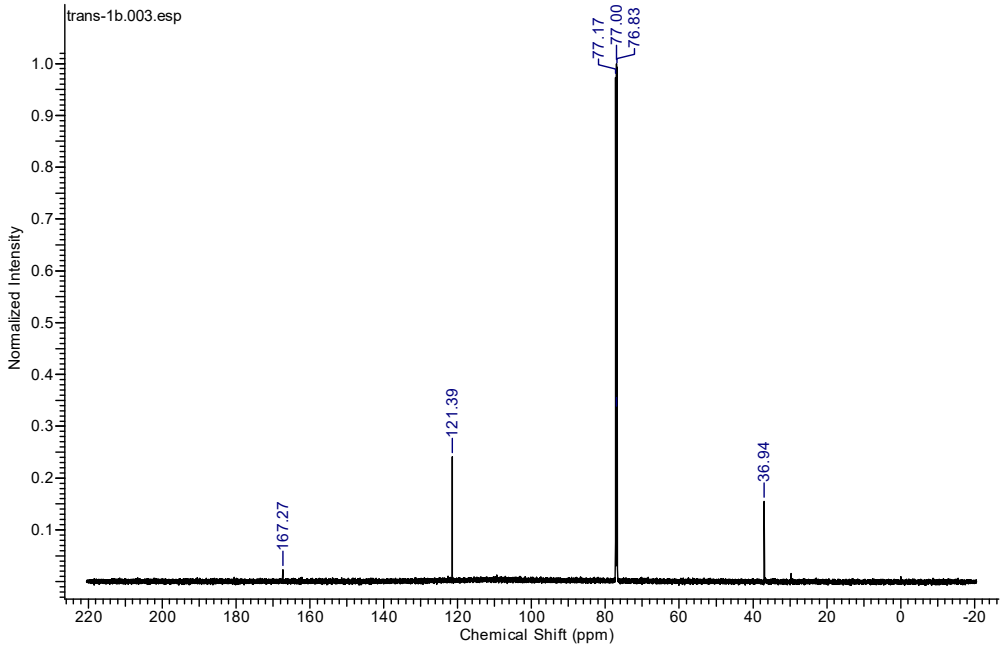

1b

Figure S1.: ^{1}H-NMR spectra ($CDCl_3$, 750 MHz) and ^{13}C-NMR spectra ($CDCl_3$, 188 MHz) of **1a** and **1b** (**1a** showed low solubility in most deuterated solvents, being slightly more soluble in chloroform-*d*)

Table S1: Structural parameters calculated. Distances (Å) and selected bond angles (°) of Compounds **1a** and **1b**.

Parameter	**DFT**		**Experimental**	
	cis-**1a**	*trans*-**1b**	*cis*-**1a**	*trans*-**1b**
C-Pt-Cl	178.40	179.88	176.75	180.0
	178.22	179.63	179.72	180.0
Pt-C	1.98	2.04	1.96	2.02
	2.41	2.39	2.36	2.31

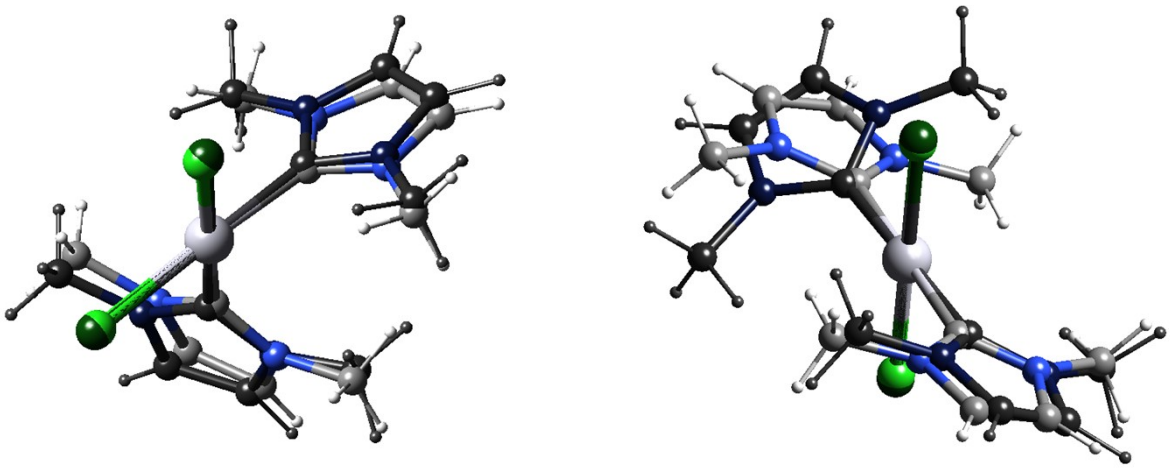

Figure S2.: Structure overlays of **1a** (left) and **1b** (right); DFT-calculated and experimental structure are shown in black and gray respectively.

Table S2. Binding energies of core electrons for **1a**, **1b,** and some reference compounds (eV). [i]N^C = 7,8-benzoquinoline; NHC = 1,3-dibenzylbenzimidazolium. *Value not reported.

	$Pt(4_{d5/2})$	**$Pt(4d_{3/2})$**	**$Pt(4f_{7/2})$**	**$Pt(4f_{5/2})$**	**Cl(2p)**	**N(1s)**	**C(1s)**	**Reference**
cis-**1a**	311.5	328.5	67.4	70.7	192.7	397.2	281.2	This work
trans-**1b**	312.5	329.5	69.1	72.4	194.8	397.3	282.1	This work
[Pt(N^C)(NHC)Br][i]	*	*	72.8	*	-	400.9	*	21
cis- $[Pt(NH_3)_2Cl_2]$	313.8	330.9	*	*	196.1	*	*	22
trans-$[Pt(NH_3)_2Cl_2]$	312.7	329.8	*	*	197.2	*	*	22

Resulting XPS spectra were deconvoluted to obtain the respective oxidation states for each element. **Platinum** 4f orbital signals remained stable during the radiation process, and no other oxidation state for the metal was observed, whereas the **Cl** 2p and **N** 1s exhibited higher sensibility to the XPS method showing the overlap of two different curves that fitted the overall signal accordingly. **C** 1s orbitals were observed as a combination of two hybridization states, where sp^3 **C** appears at a higher binding energy and aromatic carbons (sp^2) appeared shifted to the right. In figures S3a and S3b, the results after the deconvolution process are displayed; the red and yellow lines correspond to the different states that fitted the resulting spectra (black). In addition, spin-orbit states are indicated for each orbital and element analyzed.

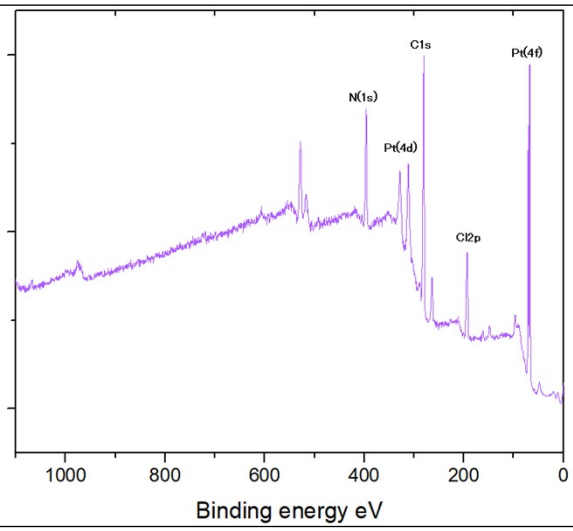

(a)

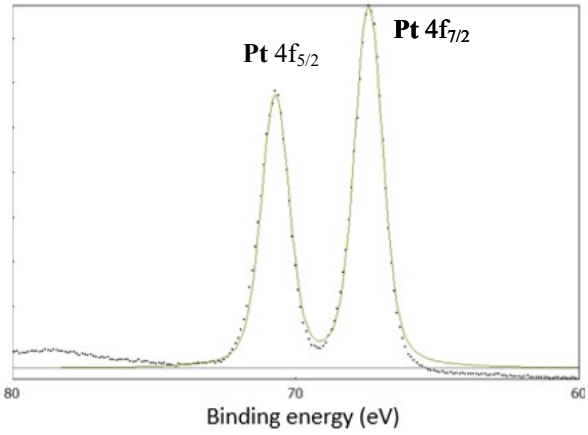

(b)

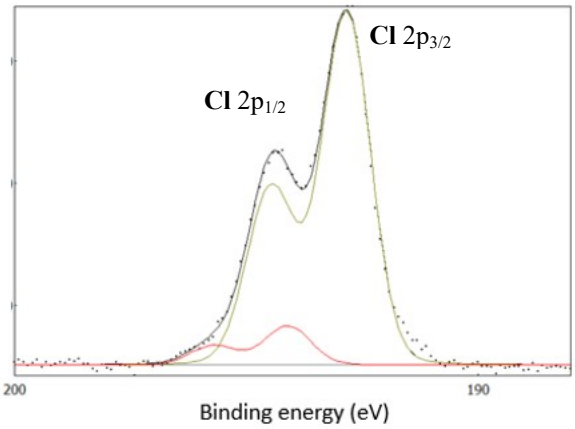

(c)

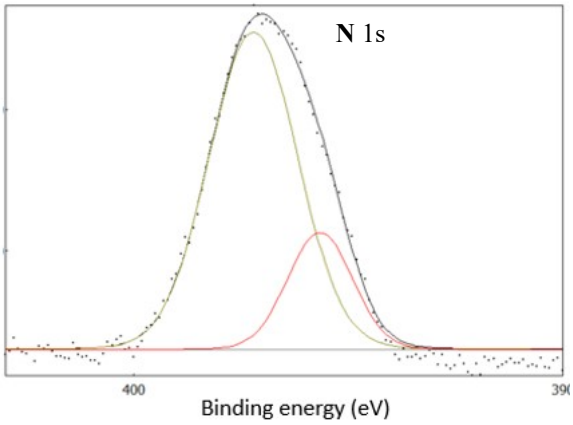

(d)

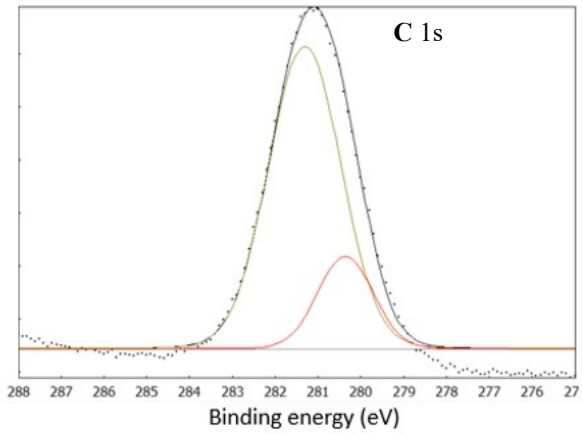

(e)

Figure S3a. X-Ray Photoelectron survey spectrum (a), and the corresponding Pt(4f), Cl(2p), N(1s) and C(1s) from (b - e) for *cis*-**1a**. Red signals correspond to different oxidation states for each element.

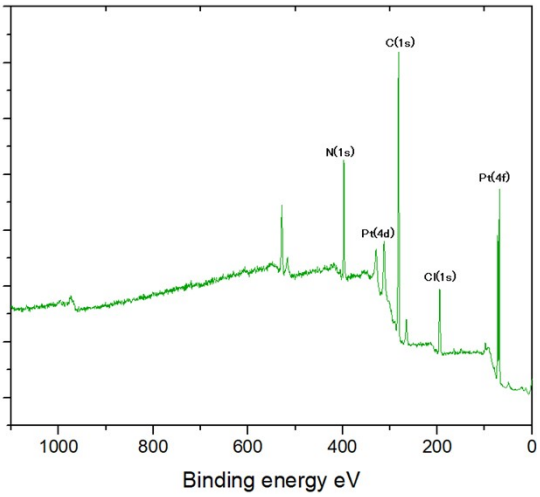

(a)

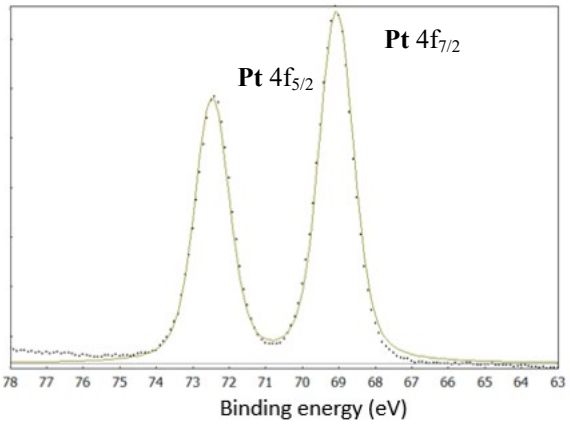

(b)

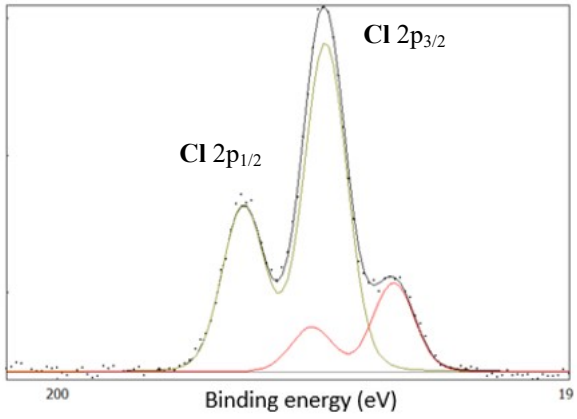

(c)

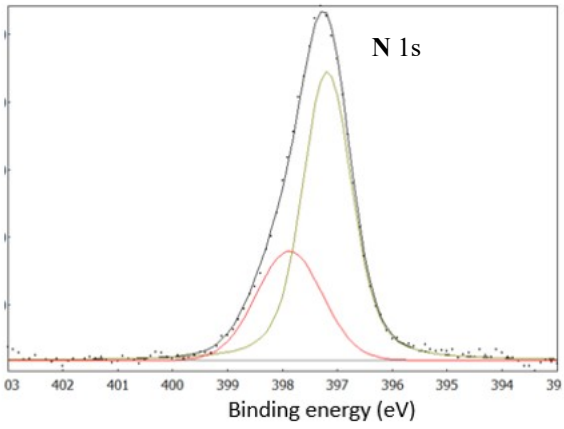

(d)

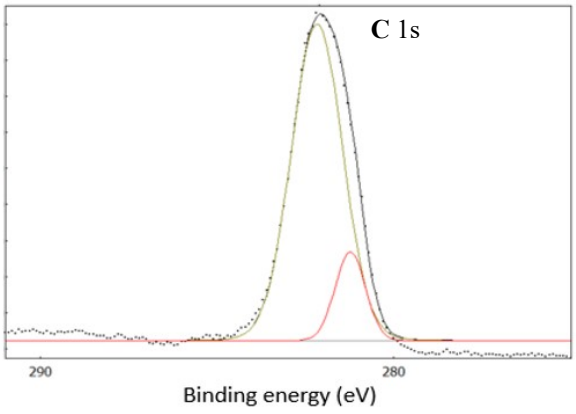

(e)

Figure S3b. *trans*-**1b** X-Ray Photoelectron survey spectrum (a), and the corresponding Pt(4f), Cl (2p), N(1s) and C(1s) from (b - e) after deconvolution. Red signals correspond to different oxidation states for each element.

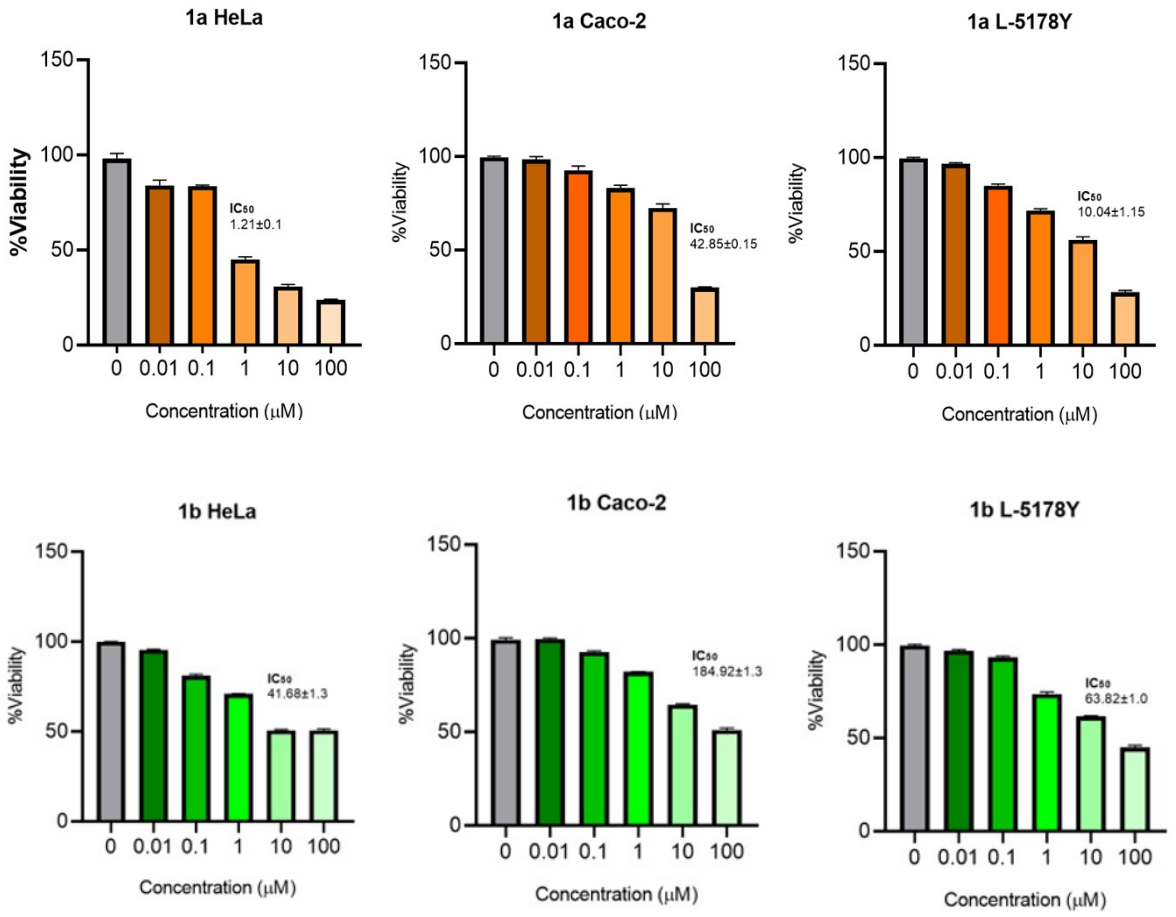

Figure S4. Graphs representing percentage of cell viability versus the concentration (μM) and IC_{50} values obtained for compounds **1a** and **1b** in all cancerous cell lines.

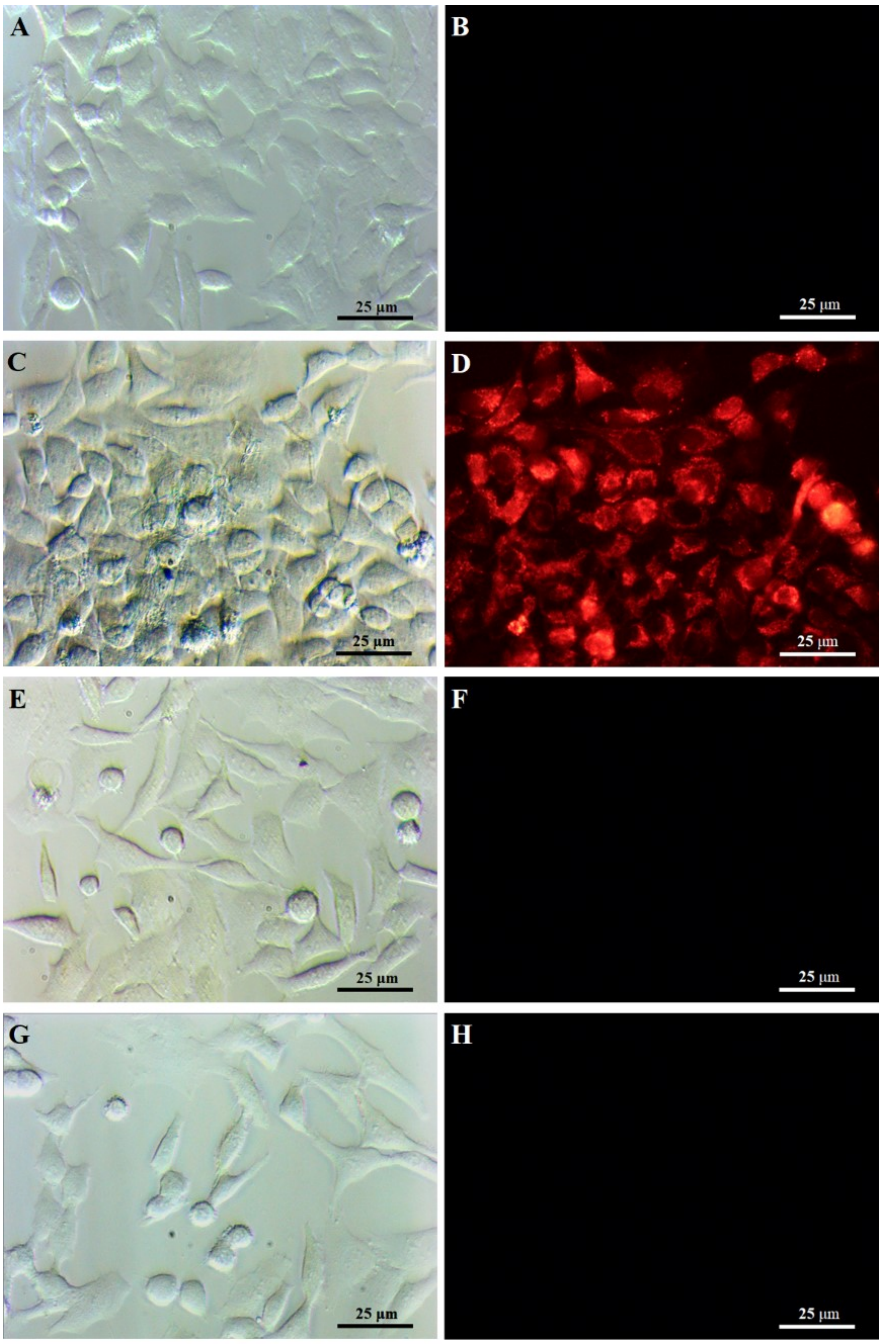

Figure S5. Phase-contrast (left) & TRITC filter (right) observations; a) and b) negative controls; c) and d) positive controls; e) y f) *cis*-**1a**/H_2O_2 group; g) y h) *trans*-**1b**/H_2O_2. Test performed in HeLa cell line.

Table S3. Zones of inhibition (ZOI) exhibited by Pt isomers at 1000 μM (units in mm).

	Gram-positive bacteria				**Gram-negative bacteria**			
Complexes	***S. aureus***	Control CMX	***B. subtilis***	Control GTM	***P. aeruginosa***	Control AMX	***E. coli***	Control PNC
1a	NI	18.3	NI	25.8	NI	23.4	7.3±0.14	22.6
1b	15.4±0.27		12.7±0.14		NI		11.0±0.15	

NI: no inhibition. ZOI are presented in milimeters. Controls used, **PNC**: Penicillin, **CMX**: Cotrimoxazole, **GTM**: Gentamicin, **AMX**: Amoxicillin.

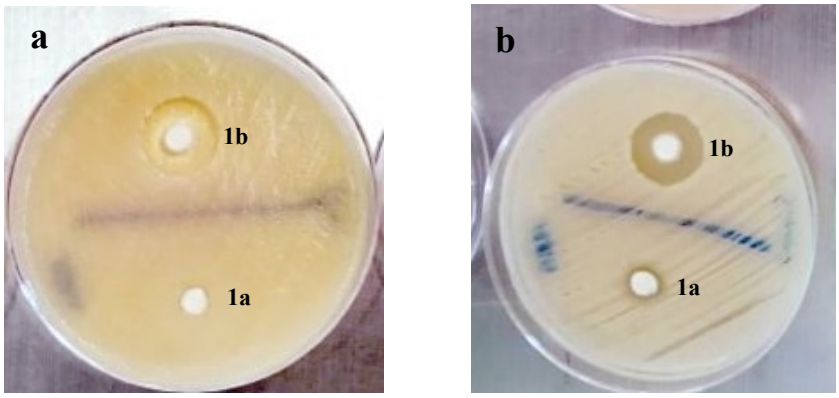

Figure S6. ZOI of 1a and 1b in: a) *S. aureus*; b) *E. coli*.

References

1 P. Van Thong, D. T. Thom and N. T. T. Chi, *Vietnam J. Chem.*, 2018, **56**, 146–151.

2 J. D. Holbrey, W. M. Reichert, I. Tkatchenko, E. Bouajila, O. Walter, I. Tommasi and R. D. Rogers, *Chem. Commun.*, 2003, **347**, 28–29.

3 O. V. Dolomanov, L. J. Bourhis, R. J. Gildea, J. A. K. Howard and H. Puschmann, *J. Appl. Crystallogr.*, 2009, **42**, 339–341.

4 G. M. Sheldrick, *Acta Crystallogr. Sect. A Found. Crystallogr.*, 2008, **64**, 112–122.

5 R. F.-M. A. M. Köster, G. Geudtner, A. Alvarez-Ibarra, P. Calaminici, M. E. Casida, J. Carmona Espíndola, F. A. Delesma, R. Delgado-Venegas, V. D. Domíinguez, J. M. G. U. Gamboa, A. Goursot, T. Heine, A. Ipatov, A. de la Lande, F. Janetzko and and D. R. S. del Campo, N. Pedroza-Montero, L. G. M. Petterson, D. Mejía-Rodríguez, J. Reveles, J. Vásquez-Pérez, A. Vela, B. A. Zúñiga-Gutiérrez, 2020.

6 G. Geudtner, P. Calaminici, J. Carmona-Espíndola, J. M. del Campo, V. D. Domínguez-Soria, R. F. Moreno, G. U. Gamboa, A. Goursot, A. M. Köster, J. U. Reveles, T. Mineva, J. M. Vásquez-Pérez, A. Vela, B. Zúñinga-Gutierrez and D. R. Salahub, *Wiley Interdiscip. Rev. Comput. Mol. Sci.*, 2012, **2**, 548–555.

7 J. P. Perdew, K. Burke and M. Ernzerhof, *Phys. Rev. Lett.*, 1996, **77**, 3865–3868.

8 J. P. Perdew, K. Burke and M. Ernzerhof, *Phys. Rev. Lett.*, 1997, **78**, 1396–1396.

9 A. M. Köster, J. U. Reveles and J. M. Del Campo, *J. Chem. Phys.*, 2004, **121**, 3417–3424.

10 N. Godbout, D. R. Salahub, J. Andzelm and E. Wimmer, *Can. J. Chem.*, 1992, **70**, 560–571.

11 P. J. Hay and W. R. Wadt, *J. Chem. Phys.*, 1985, **82**, 270–283.

12 R. Flores-Moreno, R. J. Alvarez-Mendez, A. Vela and A. M. Köster, *J. Comput. Chem.*, 2006, **27**, 1009–1019.

13 J. Andzelm, E. Radzio and D. R. Salahub, *J. Comput. Chem.*, 1985, **6**, 520–532.

14 J. Andzelm, N. Russo and D. R. Salahub, *J. Chem. Phys.*, 1987, **87**, 6562–6572.

15 P. Calaminici, F. Janetzko, A. M. Köster, R. Mejia-Olvera and B. Zuniga-Gutierrez, *J. Chem. Phys.*, , DOI:10.1063/1.2431643.

16 A. M. Köster, R. Flores-Moreno and J. U. Reveles, *J. Chem. Phys.*, 2004, **121**, 681–690.

17 J. van Meerloo, G. J. L. Kaspers and J. Cloos, in *Cancer Cell Culture*, 2011, vol. 731, pp. 237–245.

18 J. C. Stockert, A. Blázquez-Castro, M. Cañete, R. W. Horobin and Á. Villanueva, *Acta Histochem.*, 2012, **114**, 785–796.

19 A. F. Santos, D. F. Brotto, L. R. V. Favarin, N. A. Cabeza, G. R. Andrade, M. Batistote, A. A. Cavalheiro, A. Neves, D. C. M. Rodrigues and A. dos Anjos, *Rev. Bras. Farmacogn.*, 2014, **24**, 309–315.

20 J. L. Rios, M. C. Recio and A. Villar, *J. Ethnopharmacol.*, 1988, **23**, 127–149.

21 Makarova, A. A.; Grachova, E. V.; Niedzialek, D.; Solomatina, A. I.; Sonntag, S.; Fedorov, A. V.; Vilkov, O. Y.; Neudachina, V. S.; Laubschat, C.; Tunik, S. P.; Vyalikh, D. V. A *Sci. Rep.* 2016, ***6***, 1–9.

22 Roe, S. P.; Hill, J. O.; Magee, R. J. *Inorganica Chim. Acta* 1986, ***115*** (1), 20–22.